

In situ observation of liquid water evolution and transport in PEM fuel cells

Ch. Hartnig¹, I. Manke², J. Banhart², W. Lehnert¹

¹Zentrum für Sonnenenergie- und Wasserstoff-Forschung, Ulm, Germany, ²Hahn-Meitner Institute Berlin, Germany

Water management is the key problem in state-of-the-art hydrogen driven fuel cells. Considerable efforts have already been reached by new designs of flow field structures which allow a well-balanced distribution of reactants and help to avoid the formation of large amounts of liquid water. Still the performance suffers from excess water in the gas diffusion layer or drying-out phenomena, e.g. at dynamic operating conditions. These problems can be addressed by fine tuning of diffusion materials. A fundamental understanding of water distribution and transport in gas diffusion media features the key pathway to achieve the target of a well distributed water content.

Introduction:

So far, only a limited number of experimental methods are available to investigate the water evolution and transport under operating conditions. Usually, modified cells employing transparent parts used which might influence the performance as well as the water distribution in an uncontrollable way^{1,2,3,4}. One way to solve these problems has been achieved by means of neutron radiography which proved a suitable tool for in-situ investigations of water transport in the flow field channels and summarized water uptake of GDLs. Unfortunately, the spatial resolution (which is around 100 μm) is not sufficient to visualize small water cluster or even the formation of liquid water droplets inside single pores of the GDL^{5,6,7,8}.

In this contribution we report on the observation of liquid water evolution and transport in PEM fuel cell under operating conditions on a microscopic level with a resolution down to 3 μm . The achieved resolution represents an enhancement of about two orders of magnitude compared to standard neutron-based techniques. Limitations such as low resolution or strong disturbances of the system have been overcome by this method⁹. The X-ray energy was chosen such to strongly enhance the sensitivity to water. At the same time, the adsorption by the surrounding GDL material and other components was minimized.

Experimental:

A single cell setup (see Figure 1) is employed for the measurements. Serpentine type flowfields with 1mm wide channels and ribs including an electrochemically active area of 100 cm^2 were used. A cooling flowfield has been set up at the cathodic plate. The water was bypassed the respective positions to avoid additional absorption effects and ensure at the same time a proper thermal equilibration. GORE PRIMEA 5620 membrane electrode assemblies were employed for the investigations. A non-woven fiber material (SGL Carbon 10 BB) with pore sizes typically around 20-50 μm was used as GDL. Small holes were drilled in the metallic end plates. No modifications were applied to the flow field and the other components. So, the overall

impact on the water evolution and transport processes are negligible considering the fact that still the cooling flow field as well as at least one layer of thermally conductive graphite composite is around.

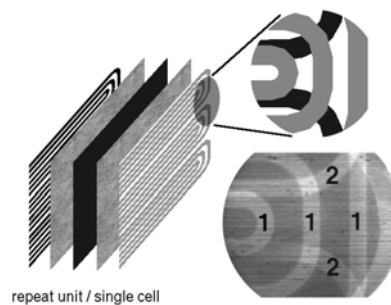


Figure 1: Left: schematic representation of a fuel cell setup including the flowfields (outermost layers), GDLs and the MEA (black layer in the center). Right - upper part: observed position in the flow field and the scheme of the radiographic output. Lower part: uncorrected radiographic image, (1): cathodic gas channel, (2): anodic gas channel.

The experiments were performed at the tomography facility of the BAMline at the Synchrotron BESSY in Berlin (Germany). An energy resolution of about $\Delta E/E = 10^{-2}$ was obtained with a monochromatic 13 keV X-ray beam. Images covering an area of 7x7 mm^2 were taken with an physical spatial resolution of 3 μm . An exposure time of 1 sec and 3.8 sec for data read-out lead to an overall measuring time per image of 4.8 sec.

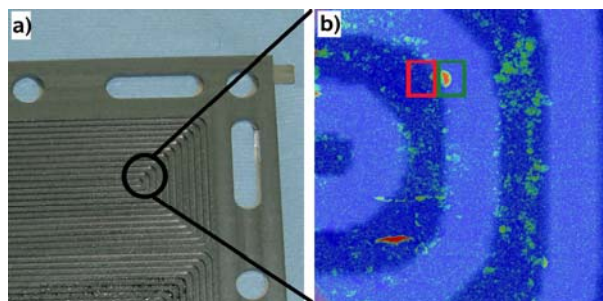


Figure 2: Left: Flow field as employed for the measurements. Right: liquid water spots in the GDL and droplet formation in the gas channels. The red and green squares are referred to in Figure 4.

The images taken under operating conditions were normalized with respect to a water-free ('dry') cell in order to turn all the other components transparent. Different operating conditions were chosen with varying current density i_0 as well as anodic utilization rates u_A to monitor the influence of the overall water content on the liquid water formation.

Results:

In Figure 3 the liquid water distributions are displayed which are observed at different operating conditions. It becomes obvious that the primary spots of liquid water evolution are located under the ribs which is in good agreement with recent theoretical findings¹⁰. The

enlargements underline these results were the area under the ribs close to the channel is water free but towards the center the amount of liquid water strongly increases. The liquid water content is quantified by means of the attenuation coefficient of water at the employed X-ray energies. A homogenous water humidification background caused by several factors which depend on the operating conditions, such as, e.g., the membrane humidification, is subtracted from each image as mentioned above.

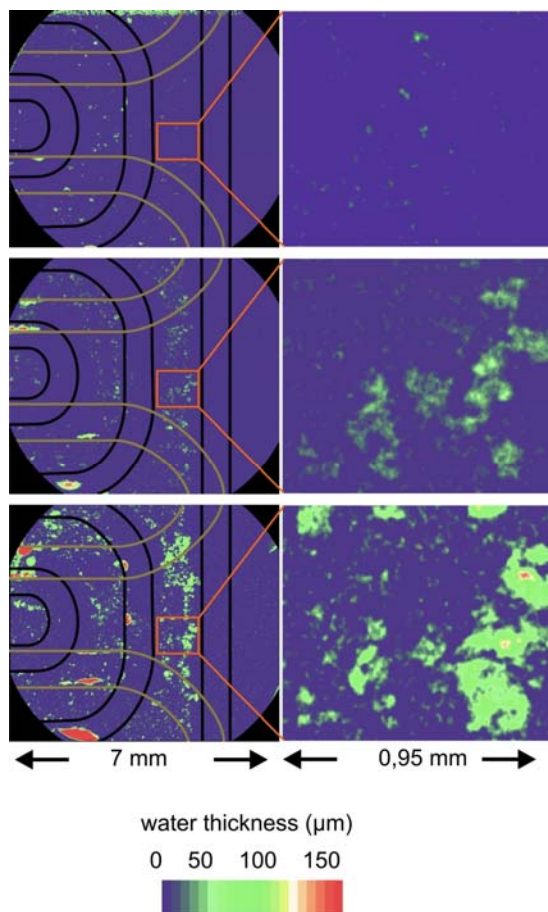


Figure 3: Liquid water formation in dependence of the operating conditions. Top: $i_0=300 \text{ mA/cm}^2$, $u_A=80\%$; middle: $i_0=500 \text{ mA/cm}^2$, $u_A=80\%$, bottom: $i_0=500 \text{ mA/cm}^2$, $u_A=97.5\%$ ($u_C=25\%$ in all cases).

At the highest current densities (and high anodic utilization rates, $u_A=97.5\%$, $i_0=500 \text{ mA/cm}^2$) many water clusters of up to $300 \mu\text{m}$ in diameter each containing up to several hundred or thousand picoliters of water can be observed (Figure 3, bottom). Based on the geometry of the gas channels, the preferred position of the water filled pores on the cathodic gas diffusion layer can be identified.

The water transport from the electrochemically active layer to the gas channel takes place in different ways. Under the channels of the flow field, almost no liquid water is observed hinting for a merely diffusive process in gas phase¹¹. Close to the ribs of the flow field, an eruptive transport mechanism was observed. The eruptive transport mechanism is characterized by an ejection of many neighboring liquid water droplets from the gas diffusion layers into the channel which was

observed recently ex-situ¹². In the channel, only one large droplet can be observed which is formed within a rather short period (far less than the observation time of 5 s).

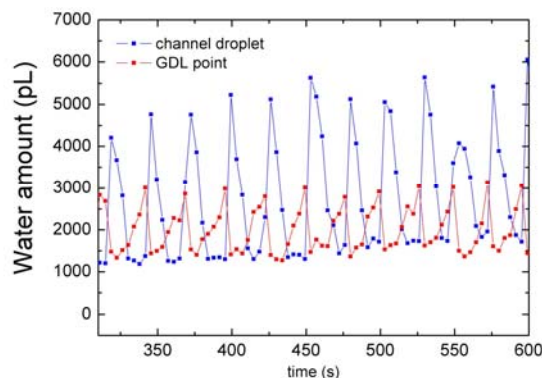


Figure 4: Time dependence of the liquid water evolution at the positions marked by squares in Figure 2 (right).

The correlated filling and eruption of two connected spots under the rib and in the gas channel (as denoted by a red resp. green square in Figure 2) is displayed in Figure 4. The red line corresponds to the filling of the GDL under the red square and the blue line to the water content of the droplet. Both show a cyclic behaviour with the same periodicity; the area under the rib is filled up to a certain pressure level; the water erupts to the channel in the next step. With increasing current densities and utilization rates the repetition times is strongly decreased.

¹ X.G. Yang, F.Y. Zhang, A.L. Lubawy, C.Y. Wang, *Electrochem. Solid-State Lett.* **7** (2004) 408

² K. Tüber, D. Pócza, C. Hebling, *J. Power Sources* **124** (2003) 403

³ F.Y. Zhang, X.G. Yang, C.Y. Wang, *J. Electrochem. Soc.* **153** (2006) 225

⁴ D. Spornjak, A. Prasad, S. Advani, *J. Power Sources* **170** (2007) 334

⁵ R.J. Bellows, M.Y. Lin, M. Arif, A.K. Thompson, D. Jacobson, *J. Electrochem. Soc.* **146** (1999) 1099

⁶ R. Satija, D.L. Jacobson, M. Arif, S.A. Werner, *J. Power Sources* **129** (2004) 238

⁷ N. Pekula, K. Heller, P.A. Chuang, A. Turhan, M.M. Mench, J.S. Brenizer, K. Ünlü, *Nucl. Instr. Methods Phys. Res. A* **542** (2005) 134

⁸ J. Zhang, D. Kramer, R. Shimoi, Y. Ono, E. Lehmann, A. Wokaun, K. Shinohara, G.G. Scherer, *Electrochim. Acta* **51** (2006) 2715

⁹ J. Baruchel, P. Cloetens, J. Härtwig, M. Schlenker, *Third-generation Hard X-Ray Synchrotron Radiation Sources*, (John Wiley & Sons, Inc., New York, 2002)

¹⁰ A.A. Kulikovskiy, T. Wüster, A. Egmen, D. Stolten, *J. Electrochem. Soc.* **152** (2005) A1290

¹¹ U. Pasaogullari, C.Y. Wang, *J. Electrochem. Soc.* **152** (2005) 380

¹² S. Litster, D. Sinton, N. Djilali, *J. Power Sources* **154** (2006) 95